Tailoring Exchange Bias through Chemical Order in Epitaxial $FePt_3$ Films

G. Mankey – University of Alabama

et al.

Citation of published version:

Saerbeck, T., et al. (2013): Tailoring Exchange Bias through Chemical Order in Epitaxial $FePt_3$ Films. *Journal of Applied Physics*, 114(1). DOI: https://doi.org/10.1063/1.4812761

Tailoring exchange bias through chemical order in epitaxial $FePt_3$ films

Cite as: J. Appl. Phys. **114**, 013901 (2013); https://doi.org/10.1063/1.4812761
Submitted: 10 June 2013 . Accepted: 18 June 2013 . Published Online: 01 July 2013

T. Saerbeck, H. Zhu, D. Lott, H. Lee, P. R. LeClair, G. J. Mankey, A. P. J. Stampfl, and F. Klose

Tailoring exchange bias through chemical order in epitaxial $FePt_3$ films

T. Saerbeck,[1,2,a),b)] H. Zhu,[1] D. Lott,[3] H. Lee,[4] P. R. LeClair,[4] G. J. Mankey,[4]
A. P. J. Stampfl,[1,5] and F. Klose[1]
[1]*Australian Nuclear Science and Technology Organisation, Menai, New South Wales 2234, Australia*
[2]*School of Physics, University of Western Australia, 35 Stirling Highway, Crawley, Western Australia 6009, Australia*
[3]*Institute for Materials Research, Helmholtz Zentrum Geesthacht, D-21502 Geesthacht, Germany*
[4]*MINT Center, University of Alabama, Tuscaloosa, Alabama 35487, USA*
[5]*School of Chemistry, The University of Sydney, New South Wales 2006, Australia*

(Received 10 June 2013; accepted 18 June 2013; published online 1 July 2013)

Intentional introduction of chemical disorder into mono-stoichiometric epitaxial $FePt_3$ films allows to create a ferro-/antiferromagnetic two-phase system, which shows a pronounced and controllable exchange bias effect. In contrast to conventional exchange bias systems, granular magnetic interfaces are created within the same crystallographic structure by local variation of chemical order. The amount of the exchange bias can be controlled by the relative amount and size of ferromagnetic and antiferromagnetic volume fractions and the interface between them. The tailoring of the magnetic composition alone, without affecting the chemical and structural compositions, opens the way to study granular magnetic exchange bias concepts separated from structural artifacts. © *2013 AIP Publishing LLC*. [http://dx.doi.org/10.1063/1.4812761]

Understanding of magnetic exchange interactions on length scales comparable to fundamental exchange distances and of the interplay between structure and magnetism is in the focus of contemporary condensed matter research aiming for modification and control of material properties.[1,2] Next to the crucial behavior of physical properties due to spatial confinement, intrinsic parameters of structural quality, chemical composition, and purity of the system play an important role. This general statement can be substantiated by the fundamental concept of magneto-electronics, which is based on scattering of conduction electrons from defects, the most apparent being the interface between two materials of different magnetizations. The interface therefore functions as an anchor point for tunability and precise control. Amongst the many phenomena of magnetic exchange coupling, the occurrence of exchange bias (EB) takes a special case and has been investigated with particular focus since its observation in the 1950s.[3,4] Phenomenologically, the effect is observed in ferromagnetic (FM)/antiferromagnetic (AFM) heterostructures as a unidirectional anisotropy shifting the magnetic hysteresis loop along the applied field axis subsequent to cooling in an applied field through the blocking temperature of the AFM/FM system.[5] Many of today's technological devices, such as data storage media and readout sensors make use of the effect, as it provides a pinning effect for a FM layer in spin-valve giant magneto-resistance multilayers.[6,7] Although it is generally agreed that the occurrence of EB is due to, but not restricted to, an interfacial pinning effect arising at the boundary between the two magnetic materials, quantitative descriptions of the effect remain a topic of controversy.[5,8] While the interface is inherently determined by structural parameters of strain, chemical alloying or interdiffusion of the bilayers, it constitutes a central ingredient for the magnitude of exchange bias.[8–10] In this report, we present an approach for removing structural elements of the interface in a granular magnetic composite system. $FePt_3$ is utilized to create a thin film with *homogeneous chemical composition* but *heterogeneous chemical order*, which leads to *heterogeneous magnetic order* and thus to the appearance of exchange bias. Depending on the growth temperature, chemical order in $FePt_3$ manifests on the atomic scale and AFM ordering replaces the FM properties present in disordered $FePt_3$ (Ref. 11) (Fig. 1(a)). As such, the system constitutes a unique way of controlling the magnetic

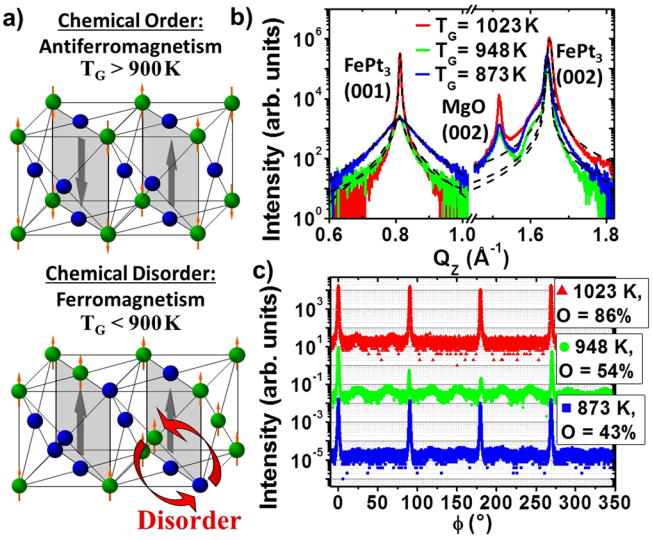

FIG. 1. Structural characterization: (a) Chemical order within crystalline $FePt_3$ (small arrows indicate the direction of the Fe moments, Pt is drawn without arrows). (b) X-ray diffraction of cubic $FePt_3$ along (001) and (002). The difference in (001) intensity determines the degree of chemical order. The dashed lines are Voigt-fits to the data. (c) ϕ-scan along (022). The 90° periodicity indicates the epitaxial growth along the cubic symmetry.

a)Electronic mail: tsaerbeck@ucsd.edu.
b)Present Address: Department of Physics, Center for Advanced Nanoscience, University of California San Diego, La Jolla, California 92093, USA

composition of a thin film without changing the materials composition, stoichiometry, or lattice structure. As demonstrated in this work, the ratio between FM and AFM volumes can be tailored, subsequently leading to a tunable EB behavior. In addition, the size and shape of magnetic domains, which in turn determines the interfacial area, can be varied independently.[12] In contrast to existing reports on the alloy $FePt_3$,[11,13–17] we concentrate on intermediate degrees of chemical order, in which controlled amounts of ordered and disordered grains coexist.

Three films of 2800 Å $FePt_3$ have been grown by magnetron sputtering from $FePt_3$ composite targets in Ar gas at a working pressure of 4×10^{-3} mbar, with a chamber base pressure of 1.3×10^{-9} mbar. Sputtering from composite targets predetermines the stoichiometric composition, which has been calibrated by Rutherford backscattering.[13,15,18] The growth temperatures, $T_G = 1023$ K, $T_G = 948$ K, and $T_G = 873$ K are based on preliminary studies with similar $FePt_3$ samples.[14,16,18] Chemically disordered $FePt_3$ crystallizes in face-centered-cubic (fcc) structure (Fig. 1(a)), in which diffraction along (001) lattice directions are structure factor forbidden. In contrast, chemical ordered $FePt_3$ shows simple-cubic symmetry and both (001) and (002) diffraction can be observed, which can be used to determine a chemical order parameter **O** using x-ray diffraction (Fig. 1(b)). The relative peak intensities of the (002) and (001) diffraction are estimated by Voigt fits. This is compared to a structural intensity calculation, in which full chemical order is assumed (**O** = 100%),[15,18] resulting in order parameters of $\mathbf{O}_{1023K} = 86 \pm 2\%$, $\mathbf{O}_{948K} = 54 \pm 4\%$, and $\mathbf{O}_{873K} = 43 \pm 3\%$ (Table I). The structural epitaxy of the films has been confirmed by x-ray ϕ-scans at the (022)-direction by rotating the sample about the surface normal. The scans show a 90° periodicity of the diffracted intensity (Figure 1(c)). In the sample grown at $T_G = 948$ K with an order parameter of **O** = 54%, a second periodicity becomes visible on a logarithmic scale, indicating a twinning of the crystalline structure. The relative extension along the out-of-plane direction of the chemically ordered phases are determined from the (001) diffraction peaks using the Scherrer formula[19] (Table I). In these calculations, the Scherrer constant was chosen to be $K = 0.94$, representing spherical objects with cubic symmetry.[20] The value for K is also the largest source for errors in determination of the absolute grain size, but a different choice, also between samples, does not affect the trend in the size distribution. Application of the Scherrer formula to the (002) peaks gave consistently high values governed by the instrumental resolution, indicating a structural coherency throughout the sample thickness.

TABLE I. Growth temperature (T_G), chemical order parameter (**O**), chemically ordered grain size (d_g), Néel temperature T_N, and exchange bias at 10 K (H_{EB}) of the three (2800 Å) $FePt_3$ thin films (Magnetic parameter is determined further below in this manuscript).

T_G (K)	**O** (%)	d_g (Å)	T_N (K)	$\mu_0 H_{EB}$ (mT)
1023	86 ± 2	871	164	−56
948	54 ± 4	138	140	−23
873	43 ± 3	44	≤140	−20

An estimate of the AFM transition temperatures is obtained performing neutron diffraction on the triple-axis-spectrometer TAIPAN at the Australian Nuclear Science and Technology Organisation, in elastic mode.[21] Figs. 2(a) and 2(b) show temperature dependent diffraction scans along the reciprocal $(0\,\frac{1}{2}\,\frac{1}{2})$-direction using monochromatic neutrons with $\lambda = 2.35$ Å. The observation of this half-order diffraction is a measure for the antiferromagnetism within the thin films according to the magnetic structure shown schematically in Fig. 1(a) (upper panel). In comparison to the diffracted intensity of the **O** = 86% sample (Fig. 2(a)), the intensity from the sample with **O** = 54% is drastically reduced and no half-order diffraction could be observed from the sample with **O** = 43%. This is related to the relative decrease in AFM material and grain size, broadening and decreasing the peak intensity below the observation limit. Diffraction along (001) from chemically ordered grains, like the case for x-rays, is not observed with neutrons due to the similarity in the nuclear scattering lengths of Fe ($b_{Fe} = 9.45 \times 10^{-5}$ Å) and Pt ($b_{Pt} = 9.6 \times 10^{-5}$ Å).[22] Second-order structural neutron diffraction along (002) and (022) was recorded at each temperature with no intensity difference being observed, discounting sample misalignment, spurious peaks or higher order wavelength contamination as the source of half-order diffraction (data not shown). In addition, no $(00\,\frac{1}{2})$ diffraction has been observed, which limits the AFM ordering to the structure shown in Fig. 1(a). The absence of a $(00\,\frac{1}{2})$-AFM phase also indicates near stoichiometric $FePt_3$ AFM grains, as an increase in Fe content leads to a second AFM transition observable below 100 K,[11] whilst an increase in Pt content effectively leads to chemical disorder. From the two samples with higher degree of ordering, a temperature dependence of the AFM diffraction is obtained (Fig. 2(c)). While a Néel temperature of $T_N(\mathbf{O} = 86\%)$

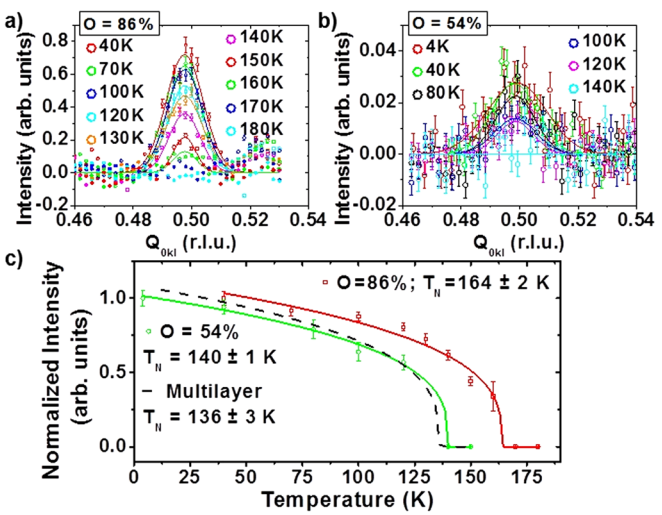

FIG. 2. High angle neutron diffraction along the $(0\,\frac{1}{2}\,\frac{1}{2})$ direction of the 2800 Å thick $FePt_3$ thin films with **O** = 86% (a) and **O** = 54% (b). Lines are Gaussian fits to the data. (c) Temperature dependence of the integrated AFM peak intensity (the line is a guide to the eye). The dashed line represents the values obtained for a $FePt_3$ order-modulated multilayer.[12]

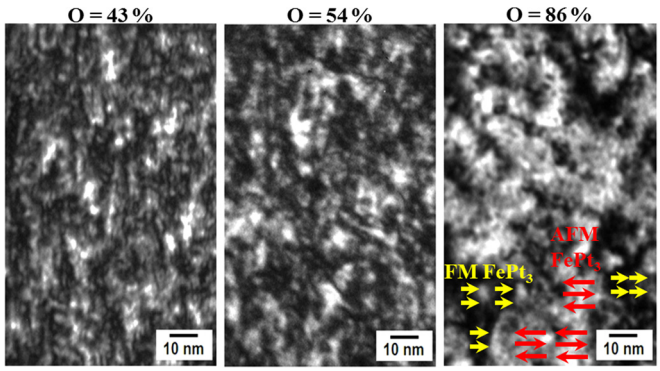

FIG. 3. Dark-field TEM images formed with a (001) diffracted beam for the cross sections of $FePt_3$ samples with different chemical order. Bright regions correspond to chemical order, while dark ones represent disordered domains. Arrows in the image for $\mathbf{O} = 86\%$ indicate the magnetic ordering within the sample's domains.

$= 164$ K is in good agreement with reported values of bulk $FePt_3$,[11,14] the $T_N(\mathbf{O} = 54\%) = 140$ K indicates a different AFM exchange stiffness in the samples with reduced order parameter and reduced grain size.

Two-dimensional information about the morphology of chemically ordered and disordered domains within the cross sections of the samples is obtained using a JEM 2200FS transmission electron microscope (TEM). Figure 3 shows dark-field (DF) TEM images of $FePt_3$ thin films for which only a (001) diffracted beam has been selected for forming the images. For the same reasons as in the x-ray diffraction, the (001) diffraction is an indication of chemical order in the material. In the DF TEM images, bright regions are identified as domains of chemical order in which the Fe moments order antiferromagnetically at low temperature. By implication, darker regions correspond to chemically disordered regions and, thus, ferromagnetic domains in the samples. The images show a mostly random shape of chemically ordered domains, which justifies the assumption of the Scherrer constant for analysis of the x-ray diffraction. Furthermore, the images highlight the evolution of the chemical order percentage as bright regions grow with increasing order parameter. The changes in the size and fraction of chemically ordered domains are consistent with the result from x-ray diffraction (Table I).

The effect of combining regions of different chemical order on the magnetic properties has been investigated using SQUID magnetometry at different temperatures. The magnetic hysteresis was recorded after field cooling in 1 T to 10 K, while the data were taken after three initial field cycles to avoid training effects.[23] Figure 4(a) shows a comparison between three samples at 10 K, showing different saturation magnetizations, different coercive fields, and EB values. The magnetization is scaled to the total $FePt_3$ volume of each sample and, thus, does not provide a direct measure of the FM magnetization. However, the decrease of the sample magnetization with increasing order parameter is in agreement with ferromagnetism only existing in chemically disordered regions. Under the assumption that the fraction of the sample showing chemical order does not contribute, the magnetization can be scaled with the order parameter. For the sample with 86% chemical order, this leads to a value, which is 13% higher than reported saturation magnetizations of $FePt_3$.[24] Values obtained for $\mathbf{O} = 54\%$ and $\mathbf{O} = 43\%$ are 50% and 40% lower than expected. This can be related to different mechanisms decreasing the observed FM magnetization. The sample with $\mathbf{O} = 86\%$ is assumed to show the largest AFM anisotropy and smallest amount of uncompensated interfacial spins, which do not contribute to the order parameter. For the other samples, the contribution of these areas increases, leading to a larger amount of spins acting paramagnetically but being attributed to chemically disordered grains. A different source of error is areas of

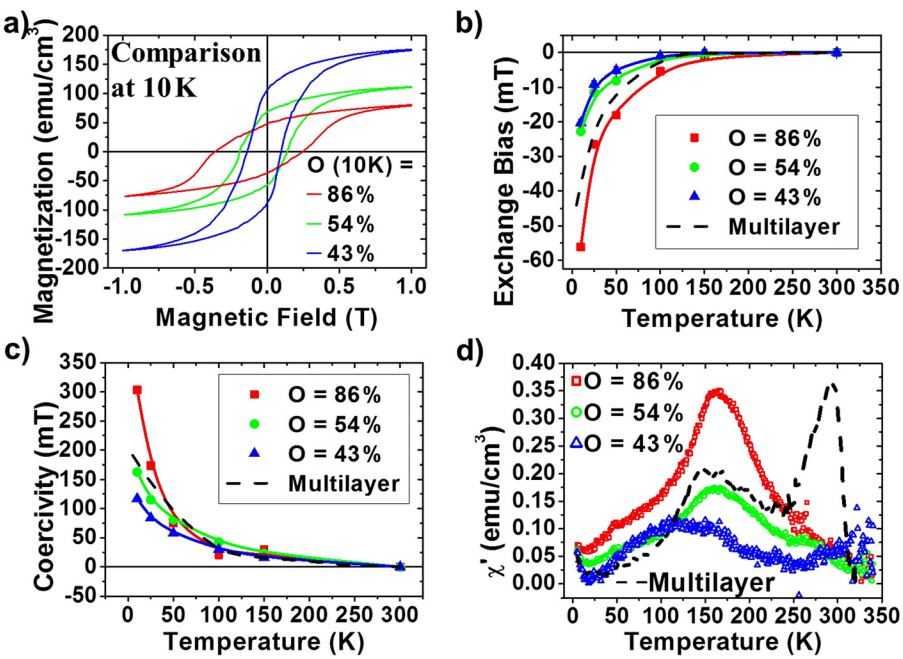

FIG. 4. Magnetic characterization: (a) magnetic hysteresis of the three samples at 10 K after field cooling in 1 T. (b) Exchange bias, determined as a shift of the hysteresis loop from the origin along the field axis. (c) Magnetic coercivity as a function of temperature. (d) AC susceptibility measured from low to high temperatures after field cooling in 1 T. The dashed lines in (b)–(d) represent the values obtained for a $FePt_3$ order-modulated multilayer.[12]

microscopic incomplete order or local stoichiometric variations, leading to different saturation magnetizations or additional paramagnetic (PM) spins. From the temperature dependence of the magnetization, a Curie temperature around 300 K is determined (data not shown), at which the hysteresis vanishes and only small paramagnetic moments are observed. EB (Fig. 4(b)) is extracted from the temperature dependent hysteresis loops as the shift of the loop center away from the field cooling direction. All samples show considerable negative EB below a temperature of 150 K, while the largest values at the lowest temperature are observed in the sample with 86% chemical ordering. Changes in the coercivity with temperature (Fig. 4(c)) show the expected scaling behavior that a larger AFM grain size leads to larger coercive fields due to an enhanced AFM anisotropy. Further magnetic characterization has been performed measuring the AC susceptibility of the films over temperature. The peaks observed around a temperature of 150 K are in agreement with the AC susceptibility associated with a PM-AFM transition, as observed earlier.[11,12,25] The intensity and width of the susceptibility peaks are related to the amount of AFM material present in the sample volume and to a distribution of AFM transition temperatures. The peak in the AC susceptibility of the lowest degree of order is substantially shifted and broadened towards lower values. The evolution of EB with order parameter shows the successful tailoring of the effect within mono-stoichiometric films. Due to the granular magentic structure of the samples, details about the magnetic mechanism responsible for the effect are difficult to obtain. For example, EB is directly dependent on the FM saturation magnetization, which can only assumed to be constant in the FM domains of all samples. Further, EB is dependent on the AFM thickness and inversely proportional to the FM layer thickness.[26,27] Both parameter change upon variation of chemical order not necessarily in a linear fashion and the contributions to the EB value can therefore not be separated. Finally, next to the total amount of interfacial area, the magnetic interface structure plays a role, as the bias is dependent on the relative orientation of AFM and FM spins on either side of the interface.[5,28,29]

The dashed lines in Figs. 4(b)–4(d) and 2(c) represent a comparison with results obtained from a chemical order-modulated $FePt_3$ multilayer with a volume averaged order parameter of $\mathbf{O}_M = 56\%$.[12] In contrast to the current study, AFM and FM domains were artificially separated in layers, rather than dispersed throughout the sample volume. While the AFM layer thickness of the multilayer ($d_g(MUL) \sim 200$ Å),[12] the total order parameter $\mathbf{O}_M$, the width of the AC susceptibility peak (Fig. 4(d)) and the Néel temperature (Fig. 2(c)) are comparable to the sample with 54% AFM grains, the observed EB is substantially increased towards lower temperatures. In addition, a peak around 300 K in the AC susceptibility shows the FM transition,[12] which is not observed for the three samples reported here. The behavior suggests that planar interfaces aid EB, which could be related to the relative orientation of AFM and FM spins. On the other hand, AFM domains in the multilayer were not resolved in the lateral direction, which could be extended and therefore provide additional AFM exchange anisotropy.

In conclusion, we have shown that chemical order in $FePt_3$ can be effectively used to tailor the exchange bias effect within a system containing only one material species. The amount of the observed EB is controlled over the amount and dispersion of relative AFM and FM domains. A well defined planar AFM/FM layering does not affect the blocking temperature, i.e., the temperature at which EB becomes observable, but increases the effect towards lower temperatures. This shows the decoupling of EB strength and blocking temperature. Such a tailoring of EB is in contrast to tuning of the effect via FM domains,[30] as the magnetic state of the FM domain is saturated in each cooling process. The approach via tailoring magnetic composition by chemical order offers the possibility to concentrate on purely magnetic effects responsible for the occurrence of the EB effect. Such an investigation needs to concentrate on the microscopic and macroscopic magnetic interface and volume effects of FM and AFM domains likewise.

H.L., P.R.L., and G.J.M. gratefully acknowledge financial support from DOE Award No. DE-FG02-08ER46499.

[1]C. H. Marrows, L. C. Chapon, and S. Langridge, Mater. Today **12**, 70 (2009).
[2]R. L. Stamps, Adv. Funct. Mater. **20**, 2380 (2010).
[3]W. H. Meiklejohn and C. P. Bean, Phys. Rev. **102**, 1413 (1956).
[4]W. H. Meiklejohn and C. P. Bean, Phys. Rev. **105**, 904 (1957).
[5]F. Radu and H. Zabel, *in Magnetic Heterostructures*, edited by H. Zabel and S. D. Bader (Springer Verlag, Berlin, 2008), Vol. 227, pp. 97–184.
[6]C. Chappert, A. Fert, and F. N. V. Dau, Nature Mater. **6**, 813 (2007).
[7]S. Parkin, X. Jiang, C. Kaiser, A. Panchula, K. Roche, and M. Samant, Proc. IEEE **91**, 661 (2003).
[8]R. L. Stamps, J. Phys. D: Appl. Phys. **33**, R247 (2000).
[9]W. Kuch, L. I. Chelaru, F. Offi, J. Wang, M. Kotsugi, and J. Kirschner, Nature Mater. **5**, 128 (2006).
[10]A. P. Malozemoff, Phys. Rev. B **35**, 3679 (1987).
[11]G. E. Bacon and J. Crangle, Proc. R. Soc. London, Ser. A **272**, 387–405 (1963).
[12]T. Saerbeck, F. Klose, D. Lott, G. J. Mankey, Z. Lu, P. R. LeClair, W. Schmidt, A. P. J. Stampfl, S. Danilkin, M. Yethiraj, and A. Schreyer, Phys. Rev. B **82**, 134409 (2010).
[13]S. Maat, O. Hellwig, G. Zeltzer, E. E. Fullerton, G. J. Mankey, M. L. Crow, and J. L. Robertson, Phys. Rev. B **63**, 134426 (2001).
[14]V. V. Krishnamurthy, I. Zoto, G. J. Mankey, J. L. Robertson, S. Maat, E. E. Fullerton, I. Nwagwu, and J. K. Akujieze, Phys. Rev. B **70**, 024424 (2004).
[15]P. Mani, V. V. Krishnamurthy, S. Maat, A. J. Kellock, J. L. Robertson, and G. J. Mankey, J. Vac. Sci. Technol. A **23**, 785 (2005).
[16]P. Mani, V. V. Krishnamurthy, J. L. Robertson, F. Klose, and G. J. Mankey, J. Appl. Phys. **99**, 08C109 (2006).
[17]N. Tobita, N. Nakajima, N. Ishimatsu, H. Maruyama, K. Shimada, H. Namatame, and M. Taniuchi, J. Phys. Soc. Jpn. **79**, 024703 (2010).
[18]Z. Lu, M. J. Walock, P. R. LeClair, G. J. Mankey, P. Mani, D. Lott, F. Klose, H. Ambaye, V. Lauter, M. Wolff, A. Schreyer, H. M. Christen, and B. C. Sales, J. Vac. Sci. Technol. A **27**, 770 (2009).
[19]B. D. Cullity, *Elements of X-ray Diffraction* (Addison-Wesley Publishing Company, Inc., Massachusetts 1956).
[20]B. E. Warren, *X-Ray Diffraction* (Dover Publications, Inc., New York, 1990).
[21]S. A. Danilkin, M. Yethiraj, T. Saerbeck, F. Klose, C. Ulrich, J. Fujioka, S. Miyasaka, Y. Tokura, and B. Keimer, J. Phys.: Conf. Ser. **340**, 012003 (2012).
[22]See http://www.ncnr.nist.gov/resources/n-lengths/ for a list of elemental neutron scattering length.
[23]A. Paul and A. Teichert, Appl. Phys. Lett. **97**, 032505 (2010).
[24]S. Maat, A. J. Kellock, D. Weller, J. E. E. Baglin, and E. E. Fullerton, J. Magn. Magn. Mater. **265**, 1 (2003).

[25]D. Lott, F. Klose, H. Ambaye, G. J. Mankey, P. Mani, M. Wolff, A. Schreyer, H. M. Christen, and B. C. Sales, Phys. Rev. B **77**, 132404 (2008).
[26]E. Fulcomer and S. H. Charap, J. Appl. Phys. **43**, 4184 (1972); **43**, 4190 (1972).
[27]J. Nogués and I. K. Schuller, J. Magn. Magn. Mater. **192**, 203 (1999).
[28]K. Takano, R. H. Kodama, A. E. Berkowitz, W. Cao, and G. Thomas, Phys. Rev. Lett. **79**, 1130 (1997).
[29]V. Baltz, B. Rodmacq, A. Zarefy, L. Lechevallier, and B. Dieny, Phys. Rev. B **81**, 052404 (2010).
[30]P. Miltényi, M. Gierlings, M. Bamming, U. May, G. Guntherodt, J. Nogues, M. Gruyters, C. Leighton, and I. K. Schuller, Appl. Phys. Lett. **75**, 2304 (1999).